Proc. 8th Int. Conf. Quarks and Nuclear Physics (QNP2018)
JPS Conf. Proc. **26**, 023008 (2019)
https://doi.org/10.7566/JPSCP.26.023008

Results of $\bar{K}NN$ Search via the (K^-, n) Reaction at J-PARC

Takumi Yamaga[1], Shuhei Ajimura[2], Hidemitsu Asano[1], George Beer[3], Carolina Berucci[4], Hyeongchan Bhang[5], Mario Bragadireanu[6], Paul Buehler[4], Luigi Busso[7,8], Michael Cargnelli[4], Seonho Choi[5], Catalina Curceanu[9], Shun Enomoto[10], Hiroyuki Fujioka[11], Yuya Fujiwara[12], Tomokazu Fukuda[14], Carlo Guaraldo[9], Tadashi Hashimoto[15,1], Ryugo S. Hayano[12], Toshihiko Hiraiwa[2], Masami Iio[10], Mihai Iliescu[9], Kentaro Inoue[2], Yosuke Ishiguro[13], Takashi Ishikawa[12], Shigeru Ishimoto[10], Kenta Itahashi[1], Masahiko Iwasaki[1,11], Koki Kanno[12], Kazuma Kato[13], Yuko Kato[1], Shingo Kawasaki[2], Paul Kienle[18],Hirofumi Kou[11], Yue Ma[1], Johann Marton[4], Yasuyuki Matsuda[12], Yutaka Mizoi[14], Ombretta Morra[7], Tomofumi Nagae[13], Hiroyuki Noumi[2], Hiroaki Ohnishi[16], Shinji Okada[1], Haruhiko Outa[1], Kristian Piscicchia[17,9], Yuta Sada[2], Atsushi Sakaguchi[2], Fuminori Sakuma[1], Masaharu Sato[10], Alessandro Scordo[9], Michiko Sekimoto[10], Hexi Shi[9], Kotaro Shirotori[2], Diana Sirghi[9,6], Florin Sirghi[9,6], Ken Suzuki[4], Shoji Suzuki[10], Takatoshi Suzuki[12], Kiyoshi Tanida[15], Hideyuki Tatsuno[19], Makoto Tokuda[11], Dai Tomono[2], Akihisa Toyoda[10], Kyo Tsukada[16], Oton Vazquez Doce[9,18], Eberhard Widmann[4], Toshimitsu Yamazaki[12,1], Qi Zhang[1], and Johann Zmeskal[4]
(J-PARC E15 Collaboration)

[1]*RIKEN, Wako, 351-0198, Japan*
[2]*Osaka University, Osaka, 567-0047, Japan*
[3]*University of Victoria, Victoria BC V8W 3P6, Canada*
[4]*Stefan-Meyer-Institut für subatomare Physik, A-1090 Vienna, Austria*
[5]*Seoul National University, Seoul, 151-742, South Korea*
[6]*National Institute of Physics and Nuclear Engineering - IFIN HH, Bucharest - Magurele, Romania*
[7]*INFN Sezione di Torino, 10125 Torino, Italy*
[8]*Universita' di Torino, Torino, Italy*
[9]*Laboratori Nazionali di Frascati dell' INFN, I-00044 Frascati, Italy*
[10]*High Energy Accelerator Research Organization (KEK), Tsukuba, 305-0801, Japan*
[11]*Tokyo Institute of Technology, Tokyo, 152-8551, Japan*
[12]*The University of Tokyo, Tokyo, 113-0033, Japan*
[13]*Kyoto University, Kyoto, 606-8502, Japan*
[14]*Osaka Electro-Communication University, Osaka, 572-8530, Japan*
[15]*Japan Atomic Energy Agency, Ibaraki 319-1195, Japan*
[16]*Tohoku University, Sendai, 982-0826, Japan*
[17]*CENTRO FERMI - Museo Storico della Fisica e Centro Studi e Ricerche "Enrico Fermi", 00184 Rome, Italy*
[18]*Technische Universität München, D-85748, Garching, Germany*
[19]*Lund University, Lund, 221 00, Sweden*

E-mail: takumi.yamaga@riken.jp

(Received June 1, 2019)

There is a long-standing argument of the existence of kaonic nucleus, which is a bound state of anti-kaon and nucleus. Theoretically, its existence is strongly supported, however its binding energy and width have not been established yet. It is strongly disired to have an experiment to investigate the simplest kaoinc nucleus, so-called K^-pp bound state. We performed an expeirment to search for K^-pp via the in-flgiht (K^-, n) reaction at J-PARC. By studing Λp invariant mass spectrum in the Λpn final state and its dependence on momentum transfer of $K^-N \to \bar{K}N$, we observed a resonant state located below M_{K^-pp} . The mass and width of this resonant state are $2324 \pm 3(stat.)^{+6}_{-3}(syst.)$ MeV/c^2, and $115 \pm 7(stat.)^{+10}_{-20}(syst.)$ MeV, respectively, which can be naturally interpreted as a theoretically predicted K^-pp bound state.

KEYWORDS: Kaonic nucelus, Kaon, Nucleus, J-PARC

1. Introduction

Interaction between an anti-kaon ($\bar{K}$) and a nucleon (N), $\bar{K}N$ interaction, has been well understood as strongly attractive force in the isospin $I = 0$ channel from experimental results of low-energy $\bar{K}$ scattering [1] and X-ray measurement from kaonic atoms [2–4]. As a consequence of this attractive interaction, there is a long-standing discussion whether the kaon can make a bound state with nucleon. The simplest case of this discussion is about a hyperon resonance of $\Lambda(1405)$. It is difficult to understand its mass by the constituent quark model (CQM) because $\Lambda(1405)$ has much smaller mass than expected by CQM among negative parity baryons. However, because its mass locates just below the $\bar{K}N$ mass-threshold ($M_{\bar{K}N} \sim 1.43$ GeV/c^2), the $\Lambda(1405)$ state can be naturally understood as a bound state of anti-kaon and nucleon in the isospin $I = 0$, namely K^-p or K^0n state. Recently, this understanding of the structure of the $\Lambda(1405)$ has been supported by lattice QCD calculation [5].

If the $\Lambda(1405)$ structure is a bound system of an anti-kaon and a nucleon with binding energy of about 20 MeV, one can be naively expected an existence of a bound system with more nucleons, which is called as kaonic nucleus. There are many theoretical calculations of kaonic nuclei in particular the simplest $\bar{K}NN$ system, so-called the K^-pp bound state. All of the theoretical calculations support the existence of the K^-pp , however, the predicted binding energies are widely distributed due to difference of energy dependence on the $\bar{K}N$ interaction in each model. Theoretical works based on phenomenological $\bar{K}N$ potential reported the binding energies of 40 - 95 MeV [6–12]. On the other hand, relatively small binding energies, in a range of 10 - 50 MeV, were predicted from theoretical calculations using a chiral SU(3)-based $\bar{K}N$ potential [11–15]. This difference of predicted binding energies is caused by lack of understanding of $\bar{K}N$ interaction in the energy region below $M_{\bar{K}N}$, which can not be directly probed by scattering experiments or X-ray measurements. Therefore, experimental study of K^-pp bound state is strongly desired to obtain an information of the $\bar{K}N$ interaction below $M_{\bar{K}N}$.

There are several experiments reporting an observation of a K^-pp candidate by using stopped-K^- reaction [16], pp collision [17], and (π^-, K^-) reaction [18]. However, another experiment using pp collision [19] and a γ-induced experiment [20] are reported that there is no evidence of K^-pp production. Thus, even its existence of the K^-pp has still not concluded yet. In order to establish the existence of K^-pp, we have studied K^-pp by using in-flight (K^-, n) reaction which is relatively simple reaction compared to other previous experiments.

2. The experiment

The J-PARC E15 experiment, which aims to search for the K^-pp bound state, was carried out at the hadron experimental facility at J-PARC. A high intense koan beam was irradiated on the ^{3}He target to produce K^-pp by the in-flight (K^-, n) reaction. In the reaction, it is natural to consider that

the K^-pp bound state is generated by a two-step reaction as follow. The incident kaon kicks out a neutron with giving its momentum, and stands around residual two protons. Then, the kaon would be captured by two protons and make a bound state. A kaon momentum of 1.0 GeV/c was chosen to maximize the reaction rate of an elementary (K^-, n) reaction. To perform this experiment, we constructed a detector system in K1.8BR beam line at J-PARC.

The detector system is composed of a beam spectrometer system, a cylindrical detector system, and a forward detector system. The beam spectrometer system contains spectrometer magnet and drift chambers measuring beam momentum, and time-of-flight detectors to identify the beam particle. The cylindrical detector system (CDS), which is constructed of cylindrical hodoscope detector and cylindrical drift chamber, can detect scattering particles which have large scattering angle from 54 to 126 degrees. This detector system is installed into a solenoid magnet providing 0.7 T magnetic field to measure momenta of detected particles. The ^{3}He target of 0.96 g/cm^2 is located the center of CDS where is the final focus point of the beam line. A forward going neutron is detected by a neutron counter of the forward detector system which is located at 15 m downstream from the ^{3}He target. A measured time-of-flight information is used for determine the neutron momentum.

We performed our first physics data taking in 2013. With this data, we observed a clear peak from the quasi-elastic (K^-, n) reaction on the ^{3}He target in the forward going neutron missing-mass spectrum [21]. This peak is well reproduced by the simulated spectra in the mass region above the K^-pp mass-threshold ($M_{K^-pp} = 2.37$ GeV/c^2). We also found that there are events below M_{K^-pp} which can not be understood as a tail of quasi-elastic peak caused by experimental resolution, nor well-known elementary processes. These events only can be produced by hyperon resonance (Y^*) production or K^-pp production processes. However, it is impossible to distinguish between them with the inclusive (K^-, n) measurement. Therefore, we performed an exclusive measurement by using CDS to identify the K^-pp decays dominantly. Theoretically, the K^-pp is expected to decay into three decay modes, Λp, $\Sigma^0 p$, and $(\pi\Sigma)^0 p$. Since the CDS only can detect charged particle, we measured the $\Lambda p \to \pi^- pp$ decay-chain. In this analysis, the kicked out neutron in the (K^-, N) reaction was not detected but kinematically identified by using missing-mass technique. This analysis method allows us to measure larger momentum transfer events than the forward neutron analysis. In the decay channel measurement, we observed a peak structure around M_{K^-pp} in the Λp invariant mass spectrum, which strongly suggests the existence of the K^-pp bound state with the binding energy of $\sim$ 20 MeV. [22]. However, we needed further investigation to confirm the peak structure and t establish the K^-pp bound state with high statistics data. To this end, we performed the second physics data taking in 2015, where about 43×10^9 kaons are irradiated on the ^{3}He target.

3. Analysis and results

To perform the measurement of $K^-pp \to \Lambda p$ decay mode, we selected events with only three particles in a reaction; Λ, proton, and kicked-out neutron. We did not require a detection of the neutron in the forward neutron detector to keep a wide coverage of acceptance of momentum transfer. Instead of this, we identified the neutron by using kinematical quantities determined by the measurement of Λp pair. For Λ, we measured the dominant decay mode, $\Lambda \to \pi^- p$, because CDS does not have a sensitivity of neutral particles. Therefore, there are three detected particles in CDS; π^- and two protons. Momenta and velocities of detected particles were obtained by curvature of its trajectory in the magnetic field and time-of-flight, respectively. Then, particle identification was performed with the obtained values together with the calculated flight length. A mass of missing particle can be calculated as a missing-mass of detected $\pi^- pp$ as shown in Fig.1. We observed a peak around 0.94 GeV/c^2 in the missing-mass spectrum which corresponds to our object; $(\Lambda p + n)$ event sample. We prepared a likelihood function to purely and efficiently select the event sample. The likelihood function is formed by DCA (distance of closest approach) informations of every trajectory and results

of kinematical fit. The fit was performed with constraints of the Λ-reconstruction mass and the four-momentum conservation of the reaction. By using the likelihood, $(\Lambda p + n)$ event sample is clearly separated from other reaction such as $\pi^- pp$+Λ or other π-production events. The purity of the selected events sample is evaluated about 70 % by using Monte Carlo simulation, where the main background comes from $\Sigma^0 pn$, and $\Sigma^- pp$ events whose contributions are about 20 % and 10 %, respectively.

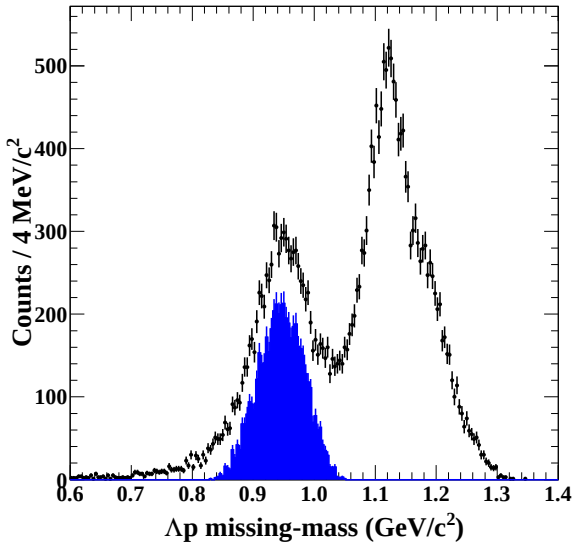

Fig. 1. Missing mass of ^{3}He$(K^-, \pi^- pp)X$ reaction. Black points show missing mass spectrum by selecting log-likelihood less than 30. Blue points are selected events as Λpn final state.

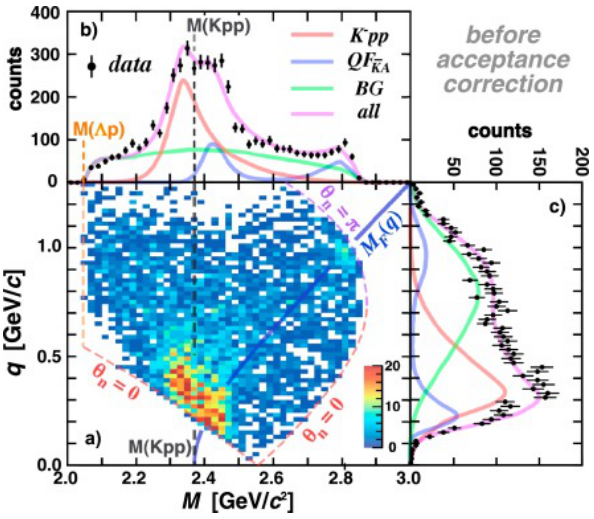

Fig. 2. 2D plot of Λp invariant mass and momentum transfer. The figure is taken from Ref. [23]. Gray curve in 2D plot shows mass dependence of the quasi-elastic kaon scattering events (Eq.1). Colored lines in projected spectra are fitting results.

With the Λpn event sample, the invariant mass of Λp pair was studied together with momentum transfer to Λp system as shown in Fig.2. The observed Λp invariant mass and momentum transfer spectra , of which statistics has been greatly improved by about 30 times,are generally consistent with our first results [22]. In the invariant mass spectrum, two peak structures are observed below and above $M_{K^- pp}$. This peak component is distributed in a low momentum transfer region which is less than 700 MeV/c. This component is strongly concentrated on the edge of kinematical limit. Also, there are another two components, a continuum contribution widely distributed in Λp three-body phase space, and an event concentration located on mass region around 2.8 GeV/c^2.

To understand the spectral shape, we attempted to decompose whole spectrum including the momentum transfer distribution. We considered following three components; resonant state, quasi-elastic contribution, and continuum component. The component of resonant state has simple Breit-Wigner shape in invariant mass distribution of which peak position does not depend on momentum transfer. We assumed S-wave Gaussian form factor to reproduce its momentum transfer distribution. The quasi-elastic contribution comes from the quasi-elastic (K^-, n) reaction on the ^{3}He target followed by conversion of $K^- + pp$ to Λp. Therefore, Λp invariant mass of this reaction (M_{QE}) is determined by the first quasi-elastic reaction which is calculated kinematically as a function of momentum transfer (q) as follows;

$$M_{QE} = \sqrt{4m_p^2 + m_K^2 + 4m_p\sqrt{m_K^2 + q^2}}, \quad (1)$$

where m_p and m_K denote mass of proton and K^-, respectively. To reproduce this contribution, we used a Gaussian distribution whose peak position has the momentum transfer dependence as described in Eq.1. This component also can explain a concentration of events on mass around 2.8 GeV/c^2 as a reaction that the kicked out neutron is scattered to backward angle in the center of mass frame of the K^- + ^{3}He reaction, i.e., the neutron is a spectator. The continuum component is widely distributed in the Λpn three-body phase space. This obsessed as component would contain many reactions, such as phase space background or physics background from $\Sigma^0 pn$ and $\Sigma^- pp$ events. In the analysis, we phenomenologically introduced a Breit-Wigner distribution with P-wave form factor with very wide width to make the distribution.

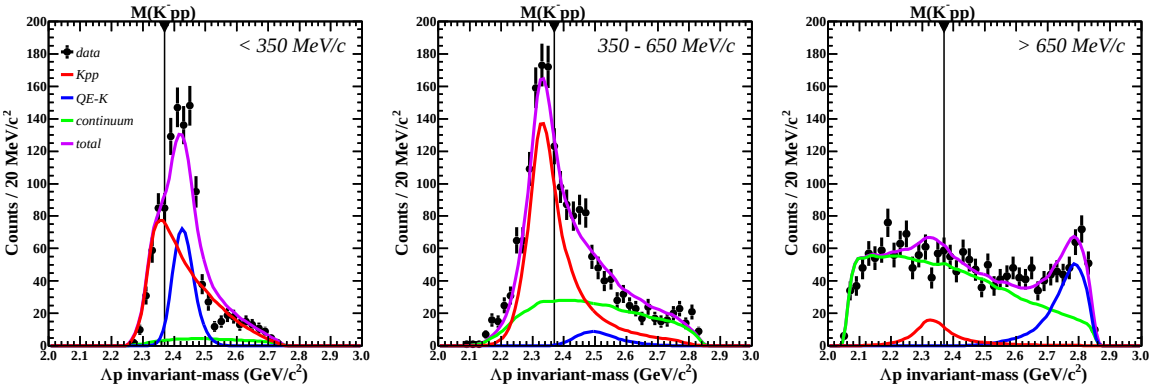

Fig. 3. Λp invariant mass spectra with selecting different momentum transfer regions of (left) less than 350 MeV/c, (middle) from 350 to 650 MeV/c, and (right) more than 650 MeV/c. Colored lines are the same fitting functions as shown in Fig.2 with selecting the same regions of momentum transfer.

The fitting result is shown in Fig.2,3. Both of the Λp invariant mass and the momentum transfer distributions are pretty well reproduced by only three simple fitting functions. The resonant state, located below M_{K^-pp} , looks to be a asymmetric shape which is far from original Breit-Wigner formula, because lower mass side of this peak goes out of a kinematical limit in a low momentum transfer region. Therefore, by selecting a low momentum transfer region of less than 350 MeV/c, the peak is strongly distorted as shown in Fig.3-(left). This distortion is getting smaller with increasing momentum transfer while recovering its original symmetric shape. Its momentum transfer distribution which is made by assuming S-wave form factor well agree with event concentration on a low momentum transfer region in the data. The quasi-elastic component has two peaks in momentum transfer spectrum, which are located around 0.2 GeV/c and 1.0 GeV/c. The momentum transfer is related to scattering angle of the kicked out neutron in the (K^-, n) reaction, hence, these two peaks correspond to the kicked out neutron going to forward (lower-q) and backward (higher-q) angles. This contribution becomes weak in middle momentum transfer region shown in Fig.3-(middle), thus the resonant component is enhanced and clearly observed in this region. In figure 3-(right), a peak made by the backward going neutron events is clearly seen around 2.8 GeV/c^2. This behavior of the quasi-elastic contribution, forward and backward peak, can be naively understood by angular distribution of the elementary (K^-, n) reaction.

As a result of this analysis, mass and decay width of the observed resonant state are evaluated to be $M = 2324\pm3(stat.)^{+6}_{-3}(syst.)$ MeV/c^2, and $\Gamma = 115\pm7(stat.)^{+10}_{-20}(syst.)$ MeV, respectively. The resonant state locates near the mass-thresholds of $M_{\Sigma(1385)p} \sim 2.32$ GeV/c^2 or $M_{\Lambda(1405)p} \sim 2.34$ MeV/c^2, thus quasi-free Y^*-production can make a structure around the peak. However, it is difficult to explain the observed peak by such quasi-free reactions, because peak position of such reactions must depends

on momentum transfer, which is similar to the case of the quasi-elastic contribution given by Eq.1. Therefore, the observed resonant state naturally considered as K^-pp. More detailed interpretation can be found in Ref. [23].

4. Conclusion

We performed an experimental study of K^-pp at J-PARC. The in-flight (K^-, n) on ^{3}He target with induced kaon momentum of 1.0 GeV/c was used to produce the K^-pp bound state. The exclusive measurement was performed to detect the expected $K^-pp \to \Lambda p$ decay mode. The observed Λp invariant mass spectrum has a peak around M_{K^-pp}. We successfully decomposed the observed spectra by performing 2-dimensional fitting of Λp invariant mass and momentum transfer. The whole spectra is well reproduced by three simple fitting functions of the K^-pp, the quasi-free component of $K^-N \to \bar{K}n$, and broad background. The mass and width of this resonant state are $2324 \pm 3(stat.)^{+6}_{-3}(syst.)$ MeV/c^2, and $115 \pm 7(stat.)^{+10}_{-20}(syst.)$ MeV, respectively, which can be naturally interpreted as a theoretically predicted K^-pp bound state.

References

[1] A. D. Martin, Nucl. Phys. B **179**, 33 (1981).
[2] M. Iwasaki, *et al.*, Phys. Rev. Lett. **78**, 3067 (1997).
[3] G. Beer, *et al.*, Phys. Rev. Lett. **94**, 212302 (2005).
[4] M. Bazzi, *et al.*, Phys. Lett.B **704**, 113 (2011).
[5] J. M. M. Hall, *et al.*, Phys. Rev. Lett. **114**, 132002 (2015).
[6] Y. Akaishi and T. Yamazaki, Phys. Rev. C **65**, 044005 (2002).
[7] T. Yamazaki and Y. Akaishi, Phys. Lett. B **535**, 70 (2002).
[8] S. Wycech and A. M. Green, Phys. Rev. C **79**, 014001 (2009).
[9] N. V. Shevchenko, Al Gal, and J. Mares, Phys. Rev. Lett. **98**, 082301 (2007).
[10] K. Ikeda and T. Sato, Phys. Rev. C **79**, 035230 (2007).
[11] S. Ohnishi, *et al.*, Phys. Rev. C **95**, 065202 (2017).
[12] K. Ikeda, H. Kamano, and T. Sato, Prog. Theor. Phys. **124**, 533 (2010).
[13] S. Ohnishi, *et al.*, Phys. Lett. B **712**, 132 (2012).
[14] A. Dote, T. Hyodo, and W. Weise, Phys. Rev. C **79**, 014003 (2009).
[15] A. Dote, T. Inoue, and T. Myo, Phys. Lett. B **784**, 405 (2018).
[16] M. Agnello, *et al.*, Phys. Rev. Lett. **94**, 212303 (2005).
[17] T. Yamazaki, *et al.*, Phys. Rev. Lett. **104**, 132502 (2010).
[18] Y. Ichikawa, *et al.*, Prog. Theor. Exp. Phys. **2015**, 021D01 (2015).
[19] G. Agakishiev, *et al.*, Phys. Lett. B **742**, 242 (2015).
[20] A. O. Tokiyasu, *et al.*, Phys. Lett. B **728**, 616 (2014).
[21] T. Hashimoto, *et al.*, Prog. Theor. Exp. Phys. **2015**, 061D01 (2015).
[22] Y. Sada, *et al.*, Prog. Theor. Exp. Phys. **2016**, 051D01 (2016).
[23] S. Ajimura, *et al.*, Phys. Lett. B **789**, 620 (2019).